Cancer Research

Genetic and Phenotypic Diversity in Breast Tumor Metastases

Vanessa Almendro[1,3,4,11], Hee Jung Kim[1,3,4,12], Yu-Kang Cheng[2,5], Mithat Gönen[8], Shalev Itzkovitz[6,13], Pedram Argani[9], Alexander van Oudenaarden[6,14], Saraswati Sukumar[10], Franziska Michor[2,5], and Kornelia Polyak[1,3,4,7]

Abstract

Metastatic disease is the main cause of cancer-related mortality due to almost universal therapeutic resistance. Despite its high clinical relevance, our knowledge of how cancer cell populations change during metastatic progression is limited. Here, we investigated intratumor genetic and phenotypic heterogeneity during metastatic progression of breast cancer. We analyzed cellular genotypes and phenotypes at the single cell level by performing immunoFISH in intact tissue sections of distant metastatic tumors from rapid autopsy cases and from primary tumors and matched lymph node metastases collected before systemic therapy. We calculated the Shannon index of intratumor diversity in all cancer cells and within phenotypically distinct cell populations. We found that the extent of intratumor genetic diversity was similar regardless of the chromosomal region analyzed, implying that it may reflect an inherent property of the tumors. We observed that genetic diversity was highest in distant metastases and was generally concordant across lesions within the same patient, whereas treatment-naïve primary tumors and matched lymph node metastases were frequently genetically more divergent. In contrast, cellular phenotypes were more discordant between distant metastases than primary tumors and matched lymph node metastases. Diversity for 8q24 was consistently higher in HER2$^+$ tumors compared with other subtypes and in metastases of triple-negative tumors relative to primary sites. We conclude that our integrative method that couples ecologic models with experimental data in human tissue samples could be used for the improved prognostication of patients with cancer and for the design of more effective therapies for progressive disease. *Cancer Res; 74(5); 1338–48. ©2014 AACR.*

Major Findings

By defining quantitative measures of intratumor cellular genetic and phenotypic heterogeneity in primary and metastatic breast tumors and by assessing tumor topology, we determined that distant metastatic tumors are the most diverse, which can explain the frequent therapy resistance of advanced stage disease.

Introduction

Metastatic dissemination and the growth of tumors at distant sites is a key step of tumor progression that is responsible for most cancer-related deaths. The accurate prediction of which patient will develop metastatic disease and the prevention and treatment of metastatic lesions remain major challenges largely due to the relative scarcity of studies of distant metastases. Difficulties associated with tissue acquisition, especially repeated sampling of multiple lesions during disease progression, and lack of faithful

Authors' Affiliations: Departments of [1]Medical Oncology and [2]Biostatistics and Computational Biology, Dana-Farber Cancer Institute; [3]Department of Medicine, Brigham and Women's Hospital; [4]Department of Medicine, Harvard Medical School; [5]Department of Biostatistics, Harvard School of Public Health, Boston; [6]Departments of Physics and Biology, Koch Institute for Integrative Cancer Research, Massachusetts Institute of Technology; [7]Harvard Stem Cell Institute, Cambridge, Massachusetts; [8]Department of Epidemiology and Biostatistics, Memorial Sloan-Kettering Cancer Center, New York, New York; Departments of [9]Pathology and [10]Oncology, Johns Hopkins University School of Medicine, Baltimore, Maryland; [11]Department of Medical Oncology, Hospital Clinic, Institut d'Investigacions Biomediques August Pi i Sunyer, Barcelona, Spain; [12]Department of Pathology, MizMedi Hospital, Seoul, South Korea; [13]Department of Molecular Cell Biology, Weizmann Institute of Science, Rehovot, Israel; and [14]Hubrecht Institute, Royal Netherlands Academy of

Arts and Sciences and University Medical Center Utrecht, Utrecht, the Netherlands

Corresponding Authors: Kornelia Polyak, Dana-Farber Cancer Institute, 450 Brookline Ave. D740C, Boston, MA 02215. Phone: 617-632-2106; Fax: 617-582-8490; E-mail: Kornelia_polyak@dfci.harvard.edu; and Franziska Michor, michor@jimmy.harvard.edu

American Association for **Cancer Research**

Quick Guide to Equations and Assumptions

$$H' = -\sum_{i=1}^{R} p_i \ln p_i, \tag{A}$$

where p_i represents the proportion of individuals belonging to the ith type or species when there are n types in total. This quantity is known as the Shannon index of diversity or Shannon entropy. This index has been widely used in the ecological literature (12). It was originally proposed by Claude Shannon to quantify the entropy (uncertainty or information content) in strings of text (13). His idea was that the more different letters there are and the more equal their proportional abundances in the string of text, the more difficult it is to correctly predict which letter will be the next one in the string. The Shannon entropy quantifies the uncertainty associated with this prediction. In ecology, p_i represents the proportion of individuals belonging to the ith species in the dataset of interest. Then the Shannon entropy quantifies the uncertainty in predicting the species identity of an individual that is taken at random from the dataset.

$$\lambda = \sum_{i=1}^{R} p_i^2 \tag{B}$$

where p_i represents the proportion of individuals belonging to the ith type or species when there are n types in total. This quantity is known as the Simpson index of diversity. The Simpson index was introduced in 1949 by Edward H. Simpson to measure the degree of concentration when individuals are classified into types (14). The square root of the index had already been introduced in 1945 by the economist Albert O. Hirschman (15). The measure equals the probability that two entities taken at random from the dataset of interest represent the same type. It also equals the weighted arithmetic mean of the proportional abundances p_i of the types of interest.

models of metastatic disease hamper progress in this area. However, a detailed molecular understanding of metastatic tumors is a prerequisite for the development of more effective cancer therapies.

In breast cancer, the risk of distant metastasis and the preferred sites for these lesions strongly correlate with tumor subtype (1). Luminal estrogen receptor positive (ER$^+$) tumors tend to have low probability of metastatic spread and preferentially form bone metastases. In contrast, Her2$^+$ and triple-negative (negative for estrogen and progesterone receptors and HER2) tumors have higher propensity for metastatic progression and form visceral and brain metastases.

Metastatic spread traditionally thought to be a late event in tumorigenesis that occurs after substantial tumor growth at the primary site (2). However, recent data in model organisms (3) and in patients with cancer (4) suggest that tumor cells may disseminate early, leading to parallel progression of primary and disseminated tumors (5), although clinically relevant distant metastases are still detected relatively late. A limited number of prior studies have analyzed the genetic profiles of primary and metastatic lesions in breast and other carcinomas and in general found a large extent of clonal relatedness between lesions (6–8). However, almost all of these studies used bulk tissue samples that do not allow for detailed characterization of clonal composition, and very few compared multiple lesions in the same patient.

Besides genetic alterations, the presence of cancer cells with more mesenchymal, stem cell–like features has been associated with increased risk of metastatic disease (9, 10); yet distant metastases are largely composed of more differentiated epithelial cells implying sequential epithelial-to-mesenchymal transition followed by mesenchymal-to-epithelial transition during dissemination and metastatic growth, respectively.

"Self-seeding" of cancer cells among multiple lesions within the same patient may also contribute to heterogeneity both within and among tumors (11). Here, we describe the combined analysis of genetic and phenotypic heterogeneity in breast cancer distant and lymph node metastases at the single cell level.

Materials and Methods

Human breast cancer samples

Formalin-fixed paraffin-embedded (FFPE) human primary tumors and metastases from patients with breast cancer were obtained from the Johns Hopkins University School of Medicine (Baltimore, MD) using protocols approved by the Institutional Review Board. Samples were de-identified before analysis. Tumor histology and expression of standard biomarkers [ER, progesterone receptor (PR), and HER2] were evaluated at the time of diagnosis according to American Society of Clinical Oncology/College of American Pathologists guidelines (16). Subtype definitions in this study were as follows: luminal A (ER$^+$ and/or PR$^+$, HER2$^-$), luminal B (ER$^+$ and/or PR$^+$, HER2$^+$), HER2$^+$ (ER$^-$, PR$^-$, and HER2$^+$), and triple negative (ER$^-$, PR$^-$, and HER2$^-$). In total, we analyzed 11 patients with distant metastases and 12 patients with matched primary tumor and lymph node metastases.

Multicolor immunoFISH

The detection of the copy number gain for 1q32.1, 8q24.13, 10p13, 11q13.2, 12p13.1, 16p13.3, and 17q21 (including the genes *NUAK2*, *NSMCE2*, *ITGA8*, *CCND1*, *H2AFJ*, *MPFL*, and *ERBB2*, respectively) and the centromeric region of each chromosome was performed using whole sections of FFPE human breast cancer tissue or breast cancer metastasis. The

tissues were dewaxed in xylene and hydrated in a series of ethanol. After heat-induced antigen retrieval overnight at 70°C in citrate buffer (pH 6), the digestion with pepsin was performed in a slide warmer at 37°C for 10 to 20 minutes depending on the sample. The immunostaining was performed at room temperature and sequentially to avoid cross-reaction between antibodies as follows: CD44 (Neomarkers, clone 156-3C11, mouse monoclonal IgG2) for 1 hour, biotin-conjugated rabbit anti-mouse IgG2a (Life Technologies; Cat#61-0240) for 30 minutes, CD24 (NeoMarkers, clone SN3b, mouse monoclonal IgM) for 1 hour, streptavidin Pacific Blue-conjugated (Life Technologies; Cat#S-11222), and Alexa Fluor 647 Goat anti-mouse IgM (Life Technologies; Cat# A-21238). The samples were then fixed in Carnoy for 10 minutes and dehydrated in a series of ethanol. The probes [bacterial artificial chromosome (BAC) probes] for the detection of 8q, 11q, 16p, 12p, 10p, and 17q were labeled with SpectrumOrange (Vysis), and the probe for the detection of 1q with SpectrumGreen (Vysis) using a Nick Translation (Abbot Molecular) according to the manufacturer's recommendations, mixed with the corresponding centromeric probe (CEP) for each chromosome (Vysis), diluted in hybridization buffer and applied to each sample. The denaturalization was performed in a slide warmer at 75°C for several minutes depending on the sample, and then the slides were incubated in a humid chamber for 20 hours at 37°C. Finally, the samples were washed with different stringent saline sodium citrate buffers, air-dried, and protected for long storage with ProLong Gold (Life Technologies). Different immunofluorescence images from multiple areas of each sample were acquired with a Nikon Ti microscope attached to a Yokogawa spinning-disk confocal unit, 60× Plan Apo objective, and OrcaER camera controlled by the Andor iQ software.

Inference of frequencies for cell phenotypes

The frequency of each phenotypically distinct cancer cell subpopulation (i.e., $CD44^+CD24^-$, $CD44^+CD24^+$, $CD44^-CD24^+$, and $CD44^-CD24^-$) was calculated by counting an average of 300 cells in each sample.

Statistical analyses

Genetic diversity was determined essentially as described (17), but we calculated diversity indices based on copy number counts for (i) BAC, (ii) chromosome-specific centromeric, (iii) ratio of BAC/CEP counts, and (iv) unique BAC and CEP count combinations. Statistical differences in primary tumor versus lymph node metastasis or between two different metastatic lesions were calculated through 100,000 iterations of bootstrapping the BAC and CEP counts from the larger cell population and comparing the mean counts of each bootstrap repetition against the mean count of the smaller cell population. Statistical differences in the BAC and CEP counts between adjacent cells in two different metastatic sites were calculated through 100,000 iterations of bootstrapping the absolute difference in BAC and CEP counts of adjacent cells from the larger cell population and comparing the mean absolute difference in counts of each bootstrap repetition against the mean absolute difference in count of the smaller cell population. Statistical

differences in BAC and CEP counts were evaluated using the achieved significance level (ASL) method (18). This amounts to using 100,000 iterations of bootstrapping the BAC and CEP counts from the larger cell population and comparing the mean counts of each bootstrap repetition against the mean count of the smaller cell population. Statistical differences in the BAC and CEP counts between adjacent cells were calculated through 100,000 iterations of bootstrapping the absolute difference in BAC and CEP counts of adjacent cells from the larger cell population and comparing the mean absolute difference in counts of each bootstrap repetition against the mean absolute difference in count of the smaller cell population. Statistical differences in the BAC and CEP counts between adjacent cells were also calculated using ASL, through 100,000 iterations of bootstrapping the absolute difference in BAC and CEP counts of adjacent cells from the larger cell population and comparing the mean absolute difference in counts of each bootstrap repetition against the mean absolute difference in count of the smaller cell population.

Topology analysis

For the analysis of the topologic distribution of cellular subsets, 3×3 images (corresponding to 71,678 μm^2 area) were obtained using 60× Plan Apo objective with 5% overlap between areas to be able to assemble them into one montage. The loci for the BAC and CEP probes were automatically detected using previously described algorithms (19). Cellular phenotype was determined manually based on immunofluorescence as described above. Both tumor and stromal cells were analyzed, and both the signals and the coordinates for each cell were recorded; however, further analysis was restricted to solely nonstromal tumor cells. For each patient, we determined the distribution of BAC and CEP counts both across all cell phenotype and independently for each phenotype. Statistical differences in the distribution of BAC and CEP counts differences between two different metastatic sites were then determined through bootstrapping. Additionally, to assess the spatial distribution of different cell phenotypes and the topologic genomic diversity we also focused on neighboring cells, which we defined as cells for which the shortest distance between cell boundaries is smaller than 10% of the average cell radius in each analyzed field of view. Significance of the differences between neighboring cells was also determined through bootstrapping. The fraction of homotypic neighbors was calculated by counting the number of pairs of neighboring cells in which both cells were the same phenotype and dividing by the total number of pairs of neighboring cells. To assess the significance of this fraction independently between two different metastatic sites, we used permutation testing. We determined the fraction of homotypic neighbors in the actual sample and compared this fraction against the fraction of homotypic neighbors in 100,000 randomized ensembles in which the cell phenotypes were randomly shuffled. The null hypothesis of this permutation test is that the pattern of homotypic neighbors seen in the sample falls within the distribution expected under random migration. A two-tailed P value was used to determine whether the fraction detected fell outside the expected range.

Figure 1. Genetic diversity in distant metastases in the same patient. A, representative images of iFISH for the indicated probes and markers. Dot plots depict Shannon diversity indices calculated based on unique BAC and CEP counts in all cancer cells combined (overall) and in phenotypically distinct tumor cell subpopulations. Dots, distinct metastatic lesions or phenotypically distinct tumor cell subpopulations within lesions. Asterisk above each tumor indicates significant differences ($P < 0.05$, statistical methodology described in Supplementary Methods). Details of tissue samples and the Shannon index of diversity calculations are listed in Supplementary Tables S1, S3, and S4, respectively. B, bar graphs, the relative frequencies of $CD44^{+}CD24^{-}$, $CD44^{+}CD24^{+}$, $CD44^{-}CD24^{+}$, and $CD44^{-}CD24^{-}$ cells in different metastases (A and B) for a given (T1–T11) patient.
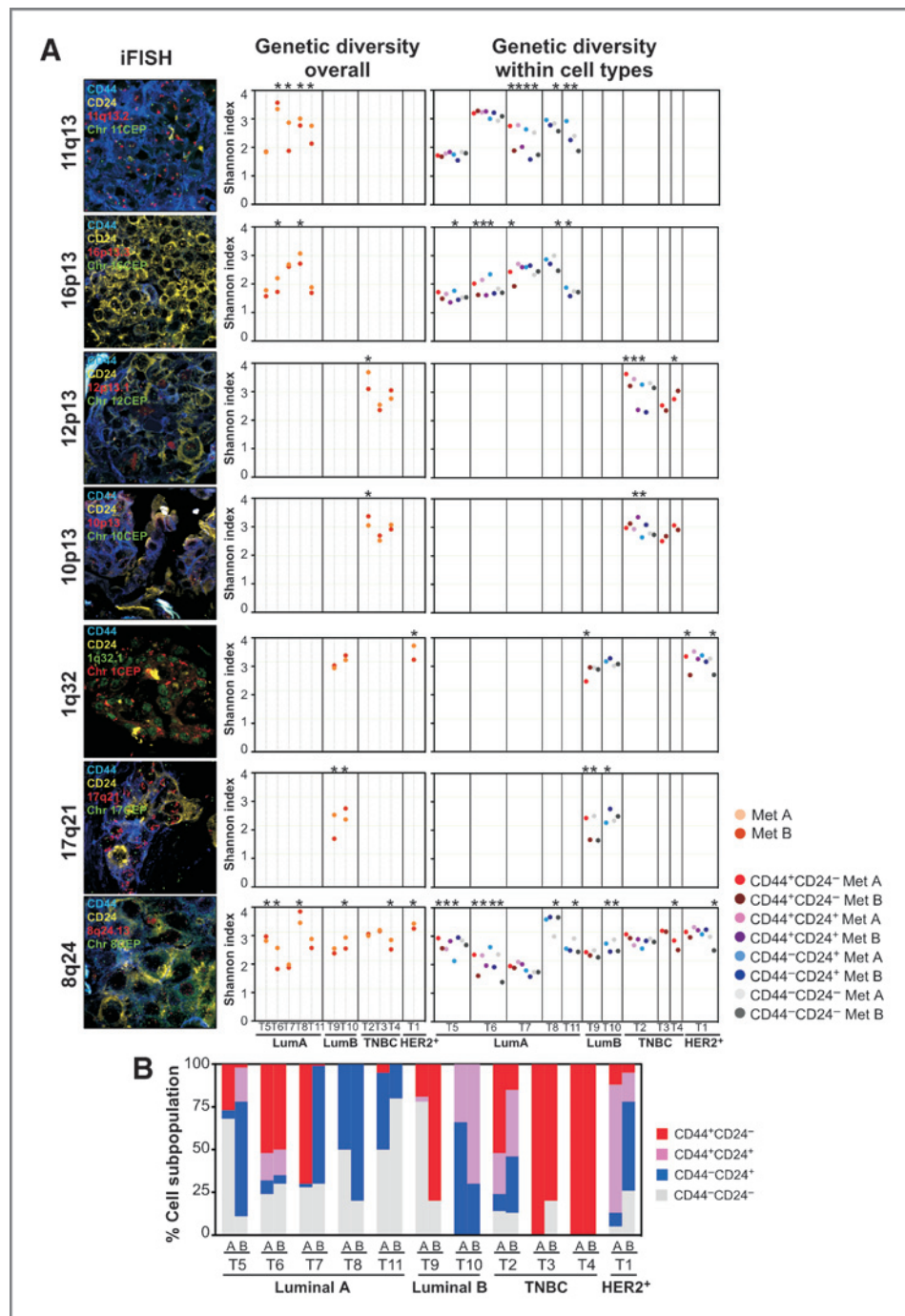
Results

Genetic and phenotypic diversity between distant metastases

To explore genetic heterogeneity in metastatic lesions from the same patient, we first performed SNP (single nucleotide polymorphism) array analysis of paired distant metastases from 11 rapid autopsies of patients with breast cancer (Supplementary Table S1; ref. 20). Overall, we detected a relatively small degree of copy number divergence between two lesions from the same patient (data not shown), potentially due to the inability of SNP arrays to detect subclonal populations within tumors when using bulk tissue samples. Thus, to obtain a more detailed picture of the subclonal structure of metastatic lesions, we performed iFISH (combined immunofluorescence and FISH; ref. 17) to assess genetic and phenotypic variability within tumors at the single cell level (Fig. 1A and Supplementary Table S1). Genetic heterogeneity was determined by evaluating copy number variation for chromosomal regions

commonly gained in each of the three major breast tumor subtypes (i.e., luminal, HER2^{+}, and triple-negative tumors; ref. 21) and corresponding CEPs. A probe for 8q24.13 was used in all tumors, for 11q13.2 and 16p13.3 in luminal, for 1q32.1 and 17q21 in HER2^{+}, and for 12p13.1 and 10p13 in triple-negative subtypes. Phenotypic heterogeneity was evaluated by staining for CD44 and CD24 cell surface markers, which identify cells with more luminal epithelial and mesenchymal features, respectively, that have different biologic properties relevant to metastasis, including invasiveness and angiogenic potential (9, 22–26). We used hematoxylin–eosine (H&E) staining to identify tumor cell-enriched areas and morphologic features to discriminate between normal and neoplastic cells. We also used autofluorescence to define tissue architecture on the FISH images and neoplastic cells

were also identifiable based on the presence of copy number gain.

Chromosomal region-specific BAC and CEP signals were counted in approximately 100 individual cells in each of the four phenotypically distinct tumor cell populations (i.e., CD44^{+}CD24^{−}, CD44^{+}CD24^{+}, CD44^{−}CD24^{+}, and CD44^{−}CD24^{−} cells; Supplementary Table S2). Overall assessment of copy number differences within phenotypically distinct cell populations in metastatic lesions revealed divergent copy number gain for multiple genomic loci in most cases (Supplementary Fig. S1); this feature was also apparent in the relative changes of unique cancer cells visualized by Kernel density and Whittaker plots (Supplementary Fig. S2; refs. 12, 17).

Next, we calculated the Shannon and Simpson indices of diversity (12) in four different ways based on measures of (i)
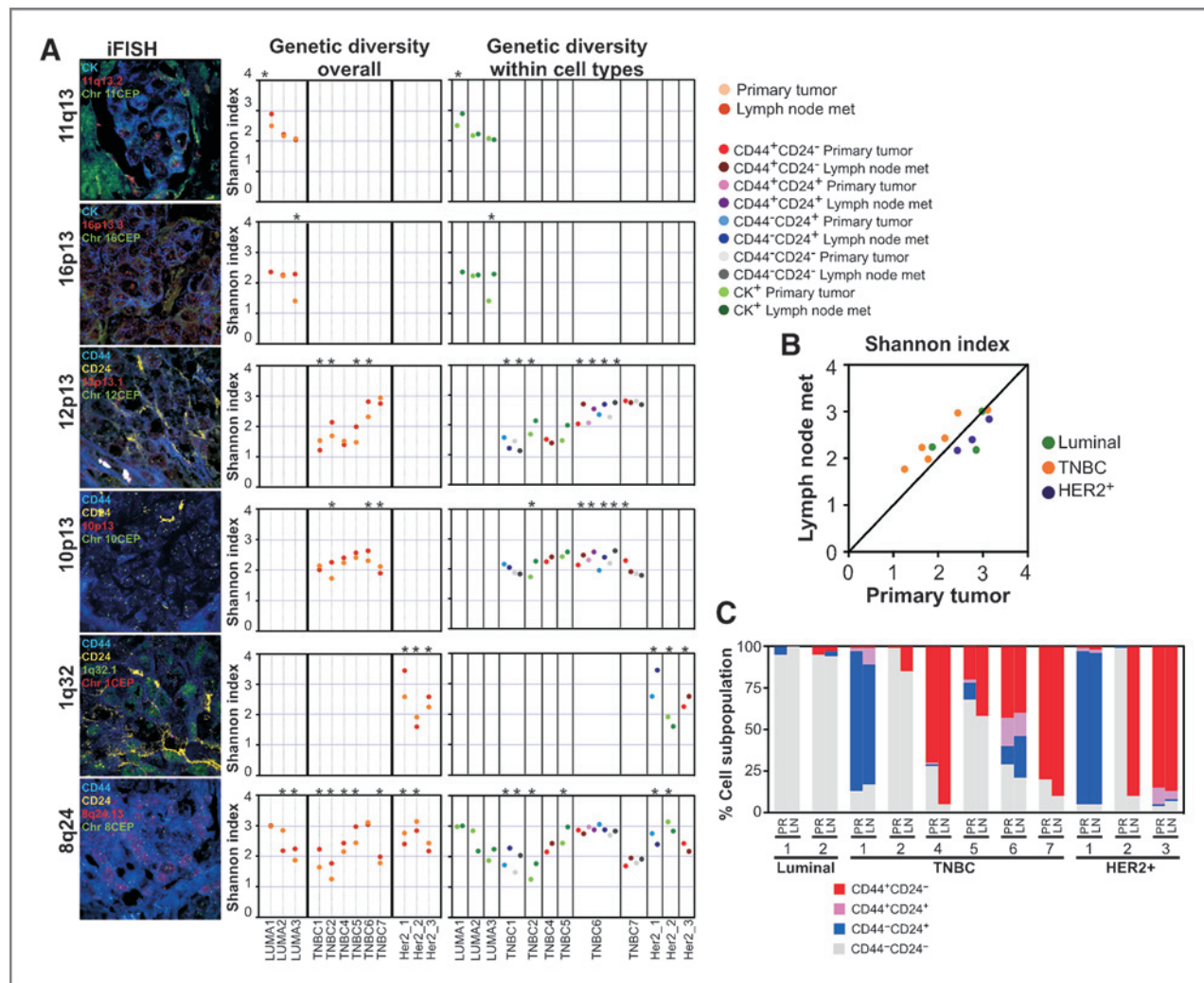

Figure 2. Genetic diversity of matched primary tumors and lymph node metastases. A, representative images of iFISH for the indicated probes and markers. Dot plots depict Shannon diversity indices calculated based on unique BAC and CEP counts in all cancer cells combined (overall) and in phenotypically distinct tumor cell subpopulations. Dots, primary tumors and lymph node metastases or phenotypically distinct tumor cell subpopulations within these lesions. Asterisk above each cell type comparison indicates significant differences ($P < 0.05$, statistical methodology described in Supplementary Methods). Details of tissue samples and the Shannon index of diversity calculations are listed in Supplementary Tables S5 and S6. B, differences in the Shannon diversity index between primary tumors and matched lymph node metastases according to breast tumor subtype. C, bar graphs, the relative frequencies of CD44^{+}CD24^{−}, CD44^{+}CD24^{+}, CD44^{−}CD24^{+}, and CD44^{−}CD24^{−} cells in matched primary tumors and lymph node metastases.

copy number of the BAC probe, (ii) copy number of the CEP, (iii) the ratio of BAC to CEP counts, and (iv) individual copy number of both BAC and CEP probes in each cell (unique counts). Overall, each of the four different calculations displayed similar relative differences among tumors, but as expected, diversity indices were highest based on unique counts (Supplementary Table S3). Measuring BAC probe and BAC to CEP ratio provides information on copy number gain of a specific locus, CEP counts alone report the degree of aneuploidy, whereas unique BAC and CEP counts provide combined information on both. Thus, to assess genetic diversity due to both copy number gain and aneuploidy, we subsequently used unique counts for all analyses unless otherwise indicated.

Overall, genetic diversity as measured by the Shannon index was significantly different between two distant metastases in the same patient for most genomic loci analyzed and in almost all cases (Fig. 1A and Supplementary Table S3). Assessment of genetic diversity within phenotypically distinct cell subpopulations provided similar results (Fig. 1A and Supplementary Table S4). However, in several cases, the differences in genetic diversity between metastatic lesions were significant only for certain loci and in specific cell populations; in some cases only one cell population showed differences and some loci were divergent only in one cell subpopulation. These results potentially reflect the order of genetic events during tumor evolution (27) or selection of a particular cell population by local microenvironmental forces. The use of the Simpson index led to similar results (Supplementary Tables S3 and S4).

To determine whether differences in cellular phenotypes contributed to the observed cell type–specific genetic diversity
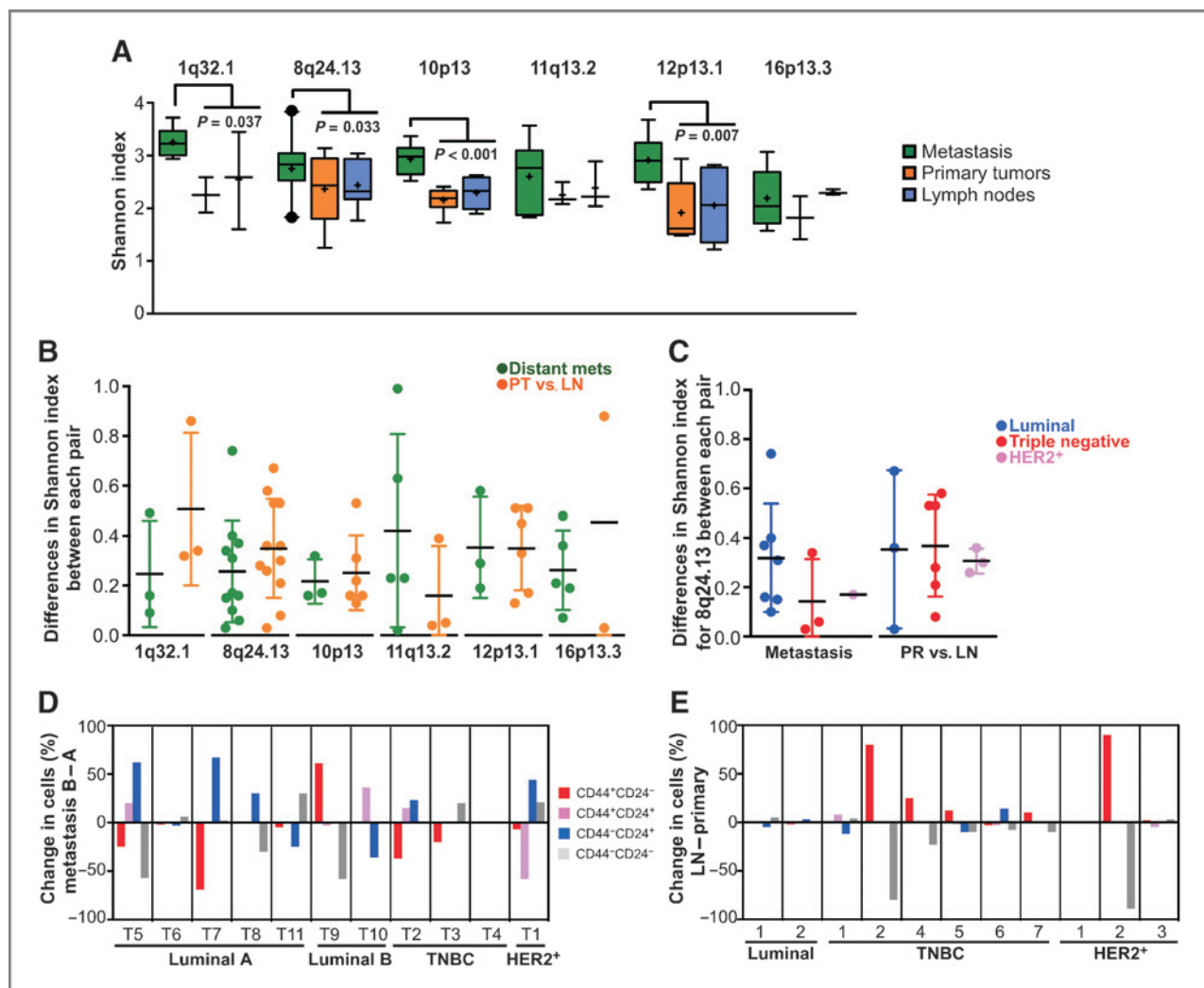

Figure 3. Differences in diversity between distant and lymph node metastases. A, box plots depict Shannon diversity indices of primary tumors and lymph node and distant metastases. Boxes show the 25th to 75th percentiles, whereas whiskers extend to the 5th and 95th percentiles. Outliers outside of the 5th and 95th percentiles are shown as black dots. Significant differences by the Mann–Whitney test between two distant metastases within the same patient and primary and lymph node metastases are shown. B, dot plots showing the differences in the Shannon index between each pair of distant metastasis or between each pair of primary and lymph node metastases for the indicated chromosomal regions. C, differences in the Shannon index for 8q24.13 in each tumor subtype. Relative changes in the frequency of each of the indicated cell population is shown in metastases (D) and in matched primary tumors and lymph node metastases (E). Details of tissue samples are listed in Supplementary Table S1. LN, lymph node metastasis.
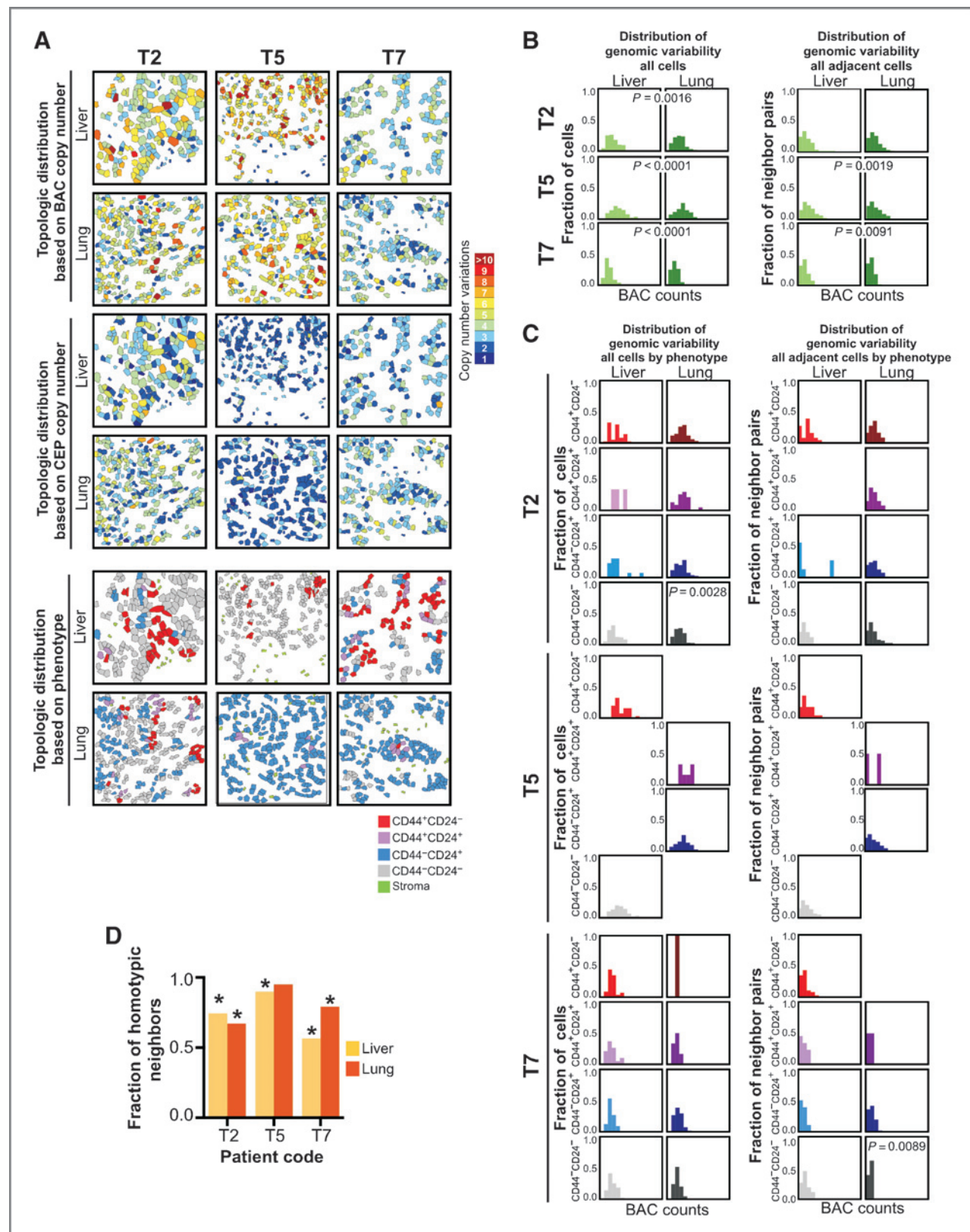
within and between metastatic lesions, we analyzed the relative frequencies of the four distinct cell subpopulations identified using CD24 and CD44 cell surface markers within tumors. Correlating with prior results from our (28) and other laboratories (29), the frequencies of the four different cell types displayed tumor subtype–specific differences, with CD44$^+$ CD24$^-$ and CD44$^-$CD24$^+$ cells being more common in triple-negative and in luminal tumors, respectively (Fig. 1B). Metastatic lesions within the same patient also displayed substantial differences in the relative frequencies of the four cell types, with the exception of two triple-negative breast cancer (TNBC) cases in which metastases were almost entirely composed of CD44$^+$CD24$^-$ cells. Interestingly, patients with TNBC had the shortest time interval from diagnosis to death implying rapid emergence and growth of distant metastases, which could potentially explain the higher similarity both for cell types and genotypes between lesions within the same patient. These results emphasize the value of combined genetic and phenotypic characterization of individual cancer cells and highlight the degree of biologic heterogeneity between metastatic lesions within the same patient.

Genetic and phenotypic diversity between primary tumors and lymph node metastases

Distant metastases in patients with breast cancer are usually detected as recurrences after systemic adjuvant therapy, making it difficult to study the natural course of the disease (30). Indeed, all patients with metastatic lesions in our cohort were diagnosed with localized tumors (T1 or T2) and many did not even have lymph node metastases at the time of diagnosis (Supplementary Table S1). Therefore, the observed high degree of genetic and phenotypic heterogeneity between metastatic lesions could be due to selection pressure by the multiple rounds of treatment the patients received. Thus, to investigate potential changes in genetic and phenotypic heterogeneity during the natural progression of breast tumors to metastatic disease, we performed iFISH analysis of primary tumors of different subtypes and matched lymph node metastases (Fig. 2A and Supplementary Tables S1 and S2) from patients who were not exposed to any systemic treatment before tissue acquisition.

In general, the extent of genetic diversity in primary tumors and lymph node metastases was lower and more variable than that observed in distant metastatic lesions, yet the differences in diversity between primary tumors and matched lymph nodes were still statistically significant in almost all cases and for all probes analyzed (Fig. 2A and Supplementary Table S5). Interestingly, TNBCs in general had lower diversity scores for 8q24, the only probe that was analyzed in all tumors, than luminal and HER2$^+$ cases, and it was consistently higher in lymph nodes compared with their matched primaries (Fig. 2B).

In contrast, diversity for 8q24 in HER2$^+$ tumors was generally high and it was higher in the primary tumors relative to matched lymph nodes.

The differences in genetic diversity were in general observed for all phenotypically distinct cell populations for most cases and probes, although for a few cases we were not able to assess all four cell types within both primary tumors and lymph node metastases (Fig. 2A and Supplementary Table S6). Thus, in contrast to distant metastatic lesions, we did not observe significant differences in diversity between primary and lymph nodes for certain cell types, potentially indicating the lack of selection for a particular phenotype. Correlating with this hypothesis, we found that the relative frequency of the four phenotypically distinct cell populations was almost identical between lymph node metastases and matched primaries (Fig. 2C).

Differences between distant and lymph node metastases

We observed several interesting differences in the genetic and phenotypic diversity of primary tumors, lymph node and distant metastases, and differences between lesions in the same patient; these findings could potentially reflect tumor evolution in unperturbed (e.g., no systemic therapy) and perturbed (cancer treatment) environments. Primary tumors and lymph node metastases had significantly lower genetic diversity for almost all chromosomal regions analyzed than distant metastases (Fig. 3A). In contrast, the difference in genetic diversity between a primary tumor and its matched lymph node metastasis was larger for some probes (e.g., 1q32 and 8q24) but smaller for others (e.g., 16p13, 11q13) than that between two distant metastases (Fig. 3B). Triple-negative tumors showed the highest differences in diversity for 8q24 between primary tumors and matched lymph nodes, whereas the opposite was observed in distant metastases (Fig. 3C). Importantly, genetic diversity indices were similar for each genomic probe analyzed (Supplementary Table S7), implying that this may reflect an inherent property of the tumor independent of the way of measurement (31).

Contrary to genetic diversity, phenotypically distinct cell populations were more commonly divergent between two distant metastases than between primary tumor and matched lymph node (Fig. 3D and E). Similar to diversity for 8q24, differences in cellular phenotypes were less pronounced between distant metastatic lesions of TNBCs than primary TNBC and its matched lymph node, whereas the opposite trend was observed for luminal tumors.

Topologic mapping of genetic and phenotypic diversity in metastasis

To further explore the impact of local microenvironments on genetic and phenotypic diversity within and between

Figure 4. Analysis of tumor topology. A, maps show topologic differences in the distribution of genetically distinct tumor cells based on copy number for 8q24 BAC, chromosome 8 CEP, and cellular phenotype in liver and lung metastases of 3 patients with breast cancer. B, histograms depicting absolute differences in copy numbers for BAC probe counts regardless of cellular phenotype in all cells or in adjacent cells in liver and lung metastases. C, histograms depicting absolute differences in copy numbers for BAC probe counts in all cells of the same phenotype or in adjacent cells of the same phenotype in liver and lung metastases. D, fraction of adjacent cells with the same phenotype in liver and lung metastases. Significance of the differences was determined by calculating the homotypic fraction for 100,000 iterations of permutation testing over randomized cellular phenotypes; *, significant differences ($P < 0.05$).

Table 1. Brief summary of the major findings

Samples	Results
Distant metastases	Genetic diversity overall is high, especially in TNBCs
	Genetic diversity indices are similar regardless of the probe used
	Two lesions in the same patients have significantly different diversity in some cases and some probes
	In some cases, genetic diversity differs between the two metastatic lesions only in some cell types
	Two lesions in the same patient are frequently phenotypically distinct except in TNBC cases
Matched primary tumors and lymph node metastases	Genetic diversity overall is lower than in distant metastases, especially true in TNBCs
	Genetic diversity indices are similar regardless of the probe used
	Genetic diversity is significantly different in most cases and most probes
	Diversity for 8q24 is lower in some primary TNBCs and higher in the lymph node metastasis
	Diversity for 8q24 is higher in some primary Her2$^+$ tumors and lower in the lymph node metastasis
	Primary and matched lymph node metastases are phenotypically more similar in most cases

tumors, we analyzed tumor topology—defined as the spatial distribution of genetically and/or phenotypically different cells within tumors–in liver and lung metastases of 3 patients. Two cases (T5 and T7) were luminal A and one (T2) was triple-negative subtype. We generated topology maps depicting individual cancer cells with specific genotypes (copy numbers for 8q24 BAC and chr8 CEP probes) and phenotypes (based on the expression of CD44 and CD24; Fig. 4A). Next, we calculated the variability for copy number in all cells and in all adjacent cancer cells (Fig. 4B and Supplementary Figs. S3A and S4). Such analysis can potentially discern different modes of tumor evolution. Large variation in all cells but low variation in adjacent cells could indicate the existence of independently evolving spatially coherent clones. In contrast, large variation between spatially adjacent cells could indicate that tumor cells are either rapidly migrating or that mutation rates are extremely high. We detected significant differences in the distribution of genetic variability in all cells and all adjacent cells of liver and lung metastases in cases T5 and T7, whereas in T2, a significant difference was only observed for all cells but not for all adjacent cells (Fig. 4B). These results may potentially indicate the differences in evolution between luminal (T5 and T7) and triple-negative (T2) tumors with the latter ones having multiple spatially independently evolving subclones.

To determine whether the differences in the distribution of genetic variability were present in all or only in some of the phenotypically distinct subpopulations, we also performed similar analyses in each of the four cell types (CD44$^+$CD24$^-$, CD44$^+$CD24$^+$, CD44$^-$CD24$^+$, and CD44$^-$CD24$^-$ cells). We observed significant differences in the distribution of genetic variability for all cells only in the CD44$^-$CD24$^-$ subpopulation in patient T2, whereas in patient T7, this was significant in all adjacent cells in the CD44$^-$CD24$^-$ population (Fig. 4C). We

also evaluated differences in the topologic distribution of cellular phenotypes and found that the frequency of homotypic interactions (i.e., adjacent cells with the same phenotype) was significantly higher compared with the frequency of heterotypic interactions between two metastatic lesions within the same patient (Fig. 4D). These data suggest that in metastatic lesions, the distribution of genetic variability is fairly even in all of the four cell types analyzed and adjacent cells are more likely to be phenotypically the same but genetically divergent.

These results again highlight the advantage of analyzing tumors *in situ* at the single cell level as tumor topology can reveal more detailed information on tumor evolution than the assessment of spatially dissociated cancer cells.

Discussion

Tumor evolution culminates in metastatic disease that is almost universally fatal due to the lack of effective therapy. Despite being the main reason of cancer-related mortality, distant metastases are still both rarely sampled and rarely subjected to molecular analyses, especially in patients with multiple metastatic lesions in different organs. Thus, our knowledge of the clonal heterogeneity of multiple lesions within the same patient is limited. Based on the traditional clonal evolution model, cancer metastases are thought to originate from a single clone present in the primary tumor, sometimes at very low frequency (2), but experimental data supporting this model are scarce. Recent high-throughput sequencing studies have attempted to address this issue and identified shared and divergent somatic variants between primary tumors and matched distant metastases in breast and pancreatic carcinomas (6, 32, 33). However, as these studies were performed on bulk tumor samples, the cellular origin and the topologic distribution of the somatic changes

could not be determined. Here, we have investigated cellular genetic and phenotypic heterogeneity in two different distant metastatic lesions from patients who failed cancer treatment as well as primary tumors and matched lymph node metastases before any systemic therapy. We determined the extent of genetic heterogeneity for chromosomal regions frequently gained in breast cancer and for cellular phenotypes associated with mesenchymal and more differentiated luminal cell features thought to be relevant to metastatic progression and therapeutic resistance. By the combined analysis of genotypes and phenotypes at the single cell level and in intact tissue slices *in situ*, we obtained a more detailed view of tumor evolution than previously possible. Table 1 lists a brief summary of our major findings.

Assessing diversity using different chromosomal regions commonly yielded different results overall or when also considering specific cellular phenotypes. These differences could be due to many reasons, including differences in the (i) acquisition of a particular genetic change during disease progression (i.e., it may reflect the order of events), (ii) genomic instability for different loci, (iii) therapeutic sensitivity of cancer cells with different copy number gain, and (iv) tumor microenvironment—both within tumors and between organs of metastatic sites.

Diversity for 8q24 was found to be significantly different between two distant metastatic lesions within the same patient in most cases both when considering the overall cell population and also when considering distinct cellular phenotypes. The same is true for primary tumors and matched lymph node metastases. The 8q24 chromosomal region harbors several important oncogenes such as C-MYC; however, 8q24 gain is almost always a reflection of gain of the whole 8q arm, thus it is difficult to determine which gene drives the selection for cancer cells with increased copy number for 8q24 (20). Copy number levels of 11q varied most often between distant metastases of luminal tumors, but not between primary tumor and lymph nodes. This amplicon contains several proliferation-related genes (e.g., CCND1), and thus, heterogeneity for this locus may result in differences in proliferation, although several of these genes also influence sensitivity to endocrine therapy (34).

Comparing the extent of diversity among lesions of different progression stages revealed that distant metastatic lesions in general have higher diversity for most loci compared with primary tumors and lymph node metastases. Distant metastases were also more commonly divergent for the relative frequency of cells with different phenotypes, although this was also influenced by tumor subtype. Interestingly, we did not see a consistent selection for a particular cellular phenotype during tumor progression; the phenotypic variability among tumors was more a reflection of tumor subtype than stage. Thus, the higher genetic and phenotypic diversity of distant metastatic tumors could be due to the multiple lines of therapy these patients received. It would be necessary to examine matched primary and distant metastatic lesions at the time of diagnosis and before any systemic therapy to differentiate between natural and treatment-induced diversity. Fortunately for patients, breast cancer is very rarely diagnosed at this late

stage; thus, the lack of such samples makes such a study difficult to conduct.

We also observed several interesting differences between tumors of different subtypes. Diversity for 8q24 was lower in primary TNBCs and increased in both distant and lymph node metastases, whereas the opposite trend was observed for HER2$^+$ cases. TNBCs are thought to metastasize at high frequency and at an earlier stage and patients with TNBC who fail treatment tend to have a shorter recurrence-free and overall survival (35). Thus, their metastatic lesions may be less likely to be divergent than those of luminal and Her2$^+$ tumors that typically have a much longer duration of disease. Luminal tumors on the other hand are slower proliferating than TNBCs and HER2$^+$ cases, which may result in lower diversity. The types of treatment given to each subtype may also influence intratumor diversity.

In summary, we found higher genetic and phenotypic diversity in distant metastases compared with primary tumors and lymph node metastases. In contrast, two different metastatic lesions were found to display lower differences in genetic diversity than a primary tumor and its matched lymph node metastasis. Because of difficulties to conduct these types of studies, the cohorts we analyzed were relatively small and the patients with metastatic lesions were autopsy cases who failed treatment. Thus, the examination of large cohorts and all stage lesions from the same patient before any systemic therapy would be necessary to conclusively determine the natural evolution of breast tumors.

Authors' Contributions

Conception and design: V. Almendro, M. Gönen, F. Michor, K. Polyak
Development of methodology: V. Almendro, H.J. Kim, Y.-K. Cheng, S. Itzkovitz
Acquisition of data (provided animals, acquired and managed patients, provided facilities, etc.): V. Almendro, P. Argani
Analysis and interpretation of data (e.g., statistical analysis, biostatistics, computational analysis): V. Almendro, H.J. Kim, Y.-K. Cheng, M. Gönen, S. Itzkovitz, A.V. Oudenaarden, F. Michor, K. Polyak
Writing, review, and/or revision of the manuscript: V. Almendro, Y.-K. Cheng, M. Gönen, P. Argani, F. Michor, K. Polyak
Administrative, technical, or material support (i.e., reporting or organizing data, constructing databases): V. Almendro, K. Polyak
Study supervision: K. Polyak

References

1. Sorlie T, Perou CM, Tibshirani R, Aas T, Geisler S, Johnsen H, et al. Gene expression patterns of breast carcinomas distinguish tumor subclasses with clinical implications. Proc Natl Acad Sci U S A 2001;98:10869–74.
2. Fearon ER, Vogelstein B. A genetic model for colorectal tumorigenesis. Cell 1990;61:759–67.
3. Weng D, Penzner JH, Song B, Koido S, Calderwood SK, Gong J. Metastasis is an early event in mouse mammary carcinomas and is associated with cells bearing stem cell markers. Breast Cancer Res 2012;14:R18.
4. Sanger N, Effenberger KE, Riethdorf S, Van Haasteren V, Gauwerky J, Wiegratz I, et al. Disseminated tumor cells in the bone marrow of patients with ductal carcinoma in situ. Int J Cancer 2011;129: 2522–6.
5. Klein CA. Parallel progression of primary tumours and metastases. Nat Rev Cancer 2009;9:302–12.
6. Yachida S, Jones S, Bozic I, Antal T, Leary R, Fu B, et al. Distant metastasis occurs late during the genetic evolution of pancreatic cancer. Nature 2010;467:1114–7.
7. Liu W, Laitinen S, Khan S, Vihinen M, Kowalski J, Yu G, et al. Copy number analysis indicates monoclonal origin of lethal metastatic prostate cancer. Nat Med 2009;15:559–65.
8. Torres L, Ribeiro FR, Pandis N, Andersen JA, Heim S, Teixeira MR. Intratumor genomic heterogeneity in breast cancer with clonal divergence between primary carcinomas and lymph node metastases. Breast Cancer Res Treat 2007;102:143–55.
9. Shipitsin M, Campbell LL, Argani P, Weremowicz S, Bloushtain-Qimron N, Yao J, et al. Molecular definition of breast tumor heterogeneity. Cancer Cell 2007;11:259–73.
10. Polyak K, Weinberg RA. Transitions between epithelial and mesenchymal states: acquisition of malignant and stem cell traits. Nat Rev Cancer 2009;9:265–73.
11. Norton L, Massague J. Is cancer a disease of self-seeding? Nat Med 2006;12:875–8.
12. Magurran AE. Measuring biological diversity. Malden: Blackwell; 2004.
13. Shannon CE. A mathematical theory of communication. Bell Syst Tech J 1948;27:379–423 and 623–56.
14. Simpson EH. Measurement of diversity. Nature 1949;163:688.
15. Hirschman AO. National power and the structure of foreign trade. Berkeley: University of California; 1945.
16. Hammond ME, Hayes DF, Wolff AC, Mangu PB, Temin S. American society of clinical oncology/college of American pathologists guideline recommendations for immunohistochemical testing of estrogen and progesterone receptors in breast cancer. J Oncol Pract 2010;6:195–7.
17. Park SY, Gönen M, Kim HJ, Michor F, Polyak K. Cellular and genetic diversity in the progression of in situ human breast carcinomas to an invasive phenotype. J Clin Invest 2010;120:636–44.
18. Efron B, Tibshirani RJ. An introduction to the bootstrap. London: Chapman & Hall; 1993.
19. Itzkovitz S, Lyubimova A, Blat IC, Maynard M, van Es J, Lees J, et al. Single-molecule transcript counting of stem-cell markers in the mouse intestine. Nat Cell Biol 2012;14:106–14.
20. Singhi AD, Cimino-Mathews A, Jenkins RB, Lan F, Fink SR, Nassar H, et al. MYC gene amplification is often acquired in lethal distant breast cancer metastases of unamplified primary tumors. Mod Pathol 2012; 25:378–87.
21. Nikolsky Y, Sviridov E, Yao J, Dosymbekov D, Ustyansky V, Kaznacheev V, et al. Genome-wide functional synergy between amplified and mutated genes in human breast cancer. Cancer Res 2008; 68:9532–40.
22. Al-Hajj M, Wicha MS, Benito-Hernandez A, Morrison SJ, Clarke MF. Prospective identification of tumorigenic breast cancer cells. Proc Natl Acad Sci U S A 2003;100:3983–8.
23. Liu R, Wang X, Chen GY, Dalerba P, Gurney A, Hoey T, et al. The prognostic role of a gene signature from tumorigenic breast-cancer cells. N Engl J Med 2007;356:217–26.
24. Li X, Lewis MT, Huang J, Gutierrez C, Osborne CK, Wu MF, et al. Intrinsic resistance of tumorigenic breast cancer cells to chemotherapy. J Natl Cancer Inst 2008;100:672–9.
25. Bloushtain-Qimron N, Yao J, Snyder EL, Shipitsin M, Campbell LL, Mani SA, et al. Cell type-specific DNA methylation patterns in the human breast. Proc Natl Acad Sci U S A 2008;105:14076–81.
26. Bloushtain-Qimron N, Yao J, Shipitsin M, Maruyama R, Polyak K. Epigenetic patterns of embryonic and adult stem cells. Cell Cycle 2009; 8:809–17.
27. Martins FC, De S, Almendro V, Gonen M, Park SY, Blum JL, et al. Evolutionary pathways in BRCA1-associated breast tumors. Cancer Discov 2012;2:503–11.
28. Park SY, Lee HE, Li H, Shipitsin M, Gelman R, Polyak K. Heterogeneity for stem cell–related markers according to tumor subtype and histologic stage in breast cancer. Clin Cancer Res 2010;16:876–87.
29. Honeth G, Bendahl PO, Ringner M, Saal LH, Gruvberger-Saal SK, Lovgren K, et al. The CD44+/CD24− phenotype is enriched in basal-like breast tumors. Breast Cancer Res 2008;10:R53.
30. Schneider C, Fehr MK, Steiner RA, Hagen D, Haller U, Fink D. Frequency and distribution pattern of distant metastases in breast cancer patients at the time of primary presentation. Arch Gynecol Obstet 2003;269:9–12.
31. Merlo LM, Shah NA, Li X, Blount PL, Vaughan TL, Reid BJ, et al. A comprehensive survey of clonal diversity measures in Barrett's esophagus as biomarkers of progression to esophageal adenocarcinoma. Cancer Prev Res (Phila) 2010;3:1388–97.
32. Shah SP, Morin RD, Khattra J, Prentice L, Pugh T, Burleigh A, et al. Mutational evolution in a lobular breast tumour profiled at single nucleotide resolution. Nature 2009;461:809–13.
33. Geyer FC, Weigelt B, Natrajan R, Lambros MB, de Biase D, Vatcheva R, et al. Molecular analysis reveals a genetic basis for the phenotypic diversity of metaplastic breast carcinomas. J Pathol 2010;220:562–73.
34. Lundgren K, Holm K, Nordenskjold B, Borg A, Landberg G. Gene products of chromosome 11q and their association with CCND1 gene amplification and tamoxifen resistance in premenopausal breast cancer. Breast Cancer Res 2008;10:R81.
35. Foulkes WD, Smith IE, Reis-Filho JS. Triple-negative breast cancer. N Engl J Med 2010;363:1938–48.